# RECENT BEAM DIAGNOSTIC TECHNIQUES

J. DIETRICH

*Forschungszentrum Jülich GmbH; Institute for Nuclear Physics, P.O. Box 19 13, D-52428 Jülich, Germany*

Recent developments in beam instrumentation and measurement techniques have been driven by technological advances, better data analysis algorithms, and the need to measure complex beam properties. New beam monitors from a wide variety of circular accelerators are briefly reviewed and a number of interesting or innovative ideas are presented in more detail. Special emphasis is given to the beam instrumentation (among others beam phase detection system, emittance measuring device, beam position monitor system) and operating experience at COSY, a cooler synchrotron and storage ring with the isochronous cyclotron JULIC as injector.

## 1 Introduction

Beam diagnostics is an essential constituent of any accelerator. A great variety of physical effects is made use of and imagination finds a wide play-ground. Today there exists a vast choice of different types of diagnostic devices and each usually in many variants. When setting out to describe a large number of diagnostic devices, one first tries to establish a systematic order. Such an approach for classification was made by H.Koziol[1].

A review of new developments of beam diagnostics in circular machines was given by G.Jackson at the EPAC 90[2]. Beam current and profile measurements as well as measurements in the transverse and longitudinal phase space are reviewed by P.Strehl[3]. An overview talk on beam instrumentation from the viewpoint not only of a producer of diagnostic equipment, but also (from the control room) of a consumer are given by S. Herb[4]. Further papers with review character are published in the proceedings of the American Beam Instrumentation Workshops[5], the Workshop on Advanced Beam Instrumentation in Tsukuba[6] and the European Workshops on Beam Instrumentation and Diagnostics for Particle Accelerators[7].

Reviewing papers submitted to recent accelerator conferences, one notes that the fields of accelerator physics and technology are becoming ever more complex and diverse. From medical accelerators to high energy physics machines, from synchrotron light sources to recirculating linacs, the beam energy, current, and sizes are dramatically different. In addition, the cycle times, revolution and RF frequencies, and geometries of these accelerators can range more than three orders of magnitude.

Thanks to advancements in high speed electronics and realtime microprocessor hardware and software beam diagnostic systems become more diverse, faster, and more intelligent.

In the following I will restrict me to some new developments in beam diagnostics for circular accelerators and transport beamlines. Special emphasis is given to the beam instrumentation of COSY, a cooler synchrotron and storage ring (momentum range 270 to 3300 MeV/c) with the isochronous cyclotron JULIC as injector[8].

## 2 Recent Developments, Tendencies, Techniques

### 2.1 *Profile and Emittance Measurements*

Optical beam monitors have been used since the early days of accelerators for observing position and shape of particle beams. In the last years the observation of beam profiles on fluorescent screens has changed from a qualitative approach to a sophisticated and quantitative method due to the availability of high quality video imaging systems and great progress in suitable software[9].

An example for such developments represents the internal beam probe for the NSCL K1200 superconducting cyclotron[10]. A probe shaft with a thin scintillator mounted on the tip and viewed by a miniature TV camera 10 cm from the scintillator is used to display the internal beam spot as function of position in the median plane. Important to notice that the camera works in a high magnetic field (up to 6 T) and in high RF power environment. Such a probe enables the operator to directly see effects of parameter adjustments on the radial and axial betatron oscillations. This is useful for detecting and correcting beam centering errors. The image gives a detailed view of the two-dimensional current density distribution with a position resolution of about 50 µm. Total beam currents below 1 epA are easily analyzed. A similar probe is installed in the INFN - LNS K800 superconducting cyclotron[11]. The high RF power environment limits the probe operation to a radius bigger than 400 mm. The scintillator plate may be removed powering a small coil interacting with the main magnetic field of the cyclotron. By this way the beam hits an insulated metallic block for total current measurement.

The enormous progress in beam image analysis systems make the "pepper pot" emittance measuring method to an interesting and more practicable tool as before[12,13]. This method uses an array of identical holes in a plate oriented in the beam transverse x-y plane. This plate is placed in the beam upstream of a beam sensitive plate (scintillating plate). The transmitted beamlets strike the plate and produce an image that is proportional to the 4-dimensional transverse phase space volume. The width of the spot is a measure of the angular divergence of the beam. The detailed intensity distribution gives the angular distribution as in the slit/grid emittance measuring method. In the past the data processing for image analysis was very time consuming. This was the reason that the "pepper pot" method was not widely used. The "pepper pot" method can deliver the 4-dimensional emittance ε (x, x', y, y'), wheras with the traditional slit/grid method the 2-dimensional emittance ε (x, x') respectively ε (y, y') are measured, of course by loosing informations.[14,15,16].

### 2.2 *Intensity Measurements*

A great variety of detectors for intensity measurements is in use around the laboratories to optimize the effficiency of particle extraction and beam transportation[17]. Especially in synchrotrons using the slow extraction mode there is a wide current range of extracted beams ($10^{-12}$ - $10^{-6}$ A, for protons corresponding to $6 \cdot 10^{6}$ - $6 \cdot 10^{12}$ pps). At the low intensity end calibration can be performed by reference to particle counters, while the high intensity end is the lower limit where beam current transformers of the fluxgate type (resolution some µA, bandwidth from dc to several kHz) can be used for calibration and nondestructive absolute particle flux measurements. At GSI Darmstadt a new type of beam current transformer using the principle of a Cryogenic Current Comperator has been developed to extend the region below 1µA down to about 1 nA[18,19]. A current of some nA produces a magnetic field in the order of $10^{-14}$ T at a distance of 10 cm. This small magnetic field is detected by a flux coupling coil with a SQUID. The main components of the detector are: a superconducting flux coupling coil as antenna for the ion beam, a coupled d.c. SQUID system as the extremely high sensitive magnetic flux sensor, a superconducting magnetic shield with a small gap, where only the azimuthal magnetic field component (proportional to the ion current) will be sensed by the pick-up coil and a special bath - cryostat with a "warm hole" (diameter 100 mm) for the passing ion beam. First tests with beam are planned in December 1995.

### 2.3 *Beam Position Measurements*

An interesting beam position monitor system is realized in CEBAF, a five pass recirculating electron accelerator, consisting of a pair of 400 MeV CW superconducting linacs connected together by two sets of five recirculating arcs stacked on top of one another[20,21,22]. All five recirculating beams occupy the same vacuum pipe in the linacs, whereas each beam has its own pipe in the arcs. Obviously, different types of beam position monitors are used in the arcs (open-ended thin wire striplines) and the linacs (short-circuited-end wire striplines). Because the accelerator is recirculating, multiple beams of different energies are present simultaneously in the linac beamlines. Two potential solutions have emerged for measuring the beam orbit in the linac sections as a function of turn number. The first technique tested at CEBAF was to modulate (100 MHz, 1µA amplitude) the bunch intensity at the injector electron gun for an interval of beam less than a recirculating time (4.2 µs) every five recirculating periods. Beam position monitors sensitive to 100 MHz then detect only the fraction of the beam on the desired recirculation orbit. The disadvantage of this technique is that a position measurement for a particular pass can only be performed once every five passes leading to an increase of time required for a complete position measurement. A similar method allowing continous signal detection for each pass is the use of pseudorandom bi-phase carrier modulation techniques. In this case the 100 MHz carrier is turned on continously but the phase of the carrier is switched in a pseudorandom fashion between 0° and 180° every recirculation period. By correlating the beam intensity waveform of the injector electron gun with the signals from the beam position monitors after a delay of $n\,\tau$ ($n = 0$ to 4, $\tau =$ recirculating time) one can measure the beam position as a function of recirculating orbit number.

### 2.4 *Signal Treatment*

Wavelets have become popular in signal analyzis applications in several fields: astronomy, image processing, filtering, theoretical physics and harmonic analysis. In the last time applications in accelerator engineering are demonstrated also[23]. Wavelets, wavelet packets and local trigonometric waveforms are collections of short oscillatory waveforms having a time duration, a frequency pitch and an amplitude. Wavelet analysis is a way to analyze a signal using base functions which are localized both in time (as diracs, but unlike sine waves) and in frequency (as sine wave, but unlike diracs). The fundamental difference between wavelet and Fourier analysis is the ability to choose a basis set. Sharply localized wavelets can resolve faster transients in a signal, while highly oscillatory wavelets can filter modulated signals quite well. There are now available software tools for wavelet analysis e.g. the program Xwpl, an graphical tool to analyze one-dimensional real-value signals using wavelets and wavelets packets under the X Window System[24].

## 3 Beam Instrumentation at COSY

### 3.1 *Cyclotron Beam Diagnostics*

#### 3.1.1 Phase Detection System of the COSY-Injector

Since the cyclotron was modified as injector for COSY, a phase detection system based on the heterodyne principle using RF-signal mixing and filtering, RF-disturbance compensating techniques and 50 Ω striplines is available to monitor continuously phase and intensity of the internal beam at 12 locations[25,26].

The equipment detects and analyzes the beam signals within a beam current range of 20 nA to 50 µA with satisfying accuracy better than 0.5°. The phase measuring system is controlled by computer and able to determine the beam phase angle and beam intensity. Furthermore the equipment includes a facility for calibrating the total beam phase detection system by a RF-signal decoupled from a dee.

The beam signals are picked up by 24 probes mounted above and below the medium plane of the cyclotron. The probes are 50 Ω striplines where the upstream end is open. The length of each probe is 15 cm, the width 15 mm and the distance between the upper and lower probes is 20 mm.

Due to the mechanical width of 15 mm the pickups take - depending on radius - beam signals from about 2 to 9 beam orbits. This results in a measured sensitivity of about 100 μV/μA (DC beam current). 12 independent pickup pairs are used together with 12 parallel operation phase detection channels.

All 12 channels can be read out in parallel without channel multiplexing. Thus the beam phase can be measured in continuous as well as in pulsed beam mode. The shortest pulse width is approximately 5 ms. An extra pickup mounted on the dee provides the possibility to eliminate phase response differences between the 12-RF-signal handling channels and a reference channel for calibrating the system to the beam zero phase. The phase detection system works over the full cyclotron frequency range from 20 to 30 MHz.

The original configuration of the system was modified in one respect: Since not all 12 internal phase probes are necessary one electronic channel was connected to a capacitive probe in the injection beamline to COSY. This allows detection of the external beam current and hence the monitoring of the extraction efficiency of the cyclotron.

Changes of the injection efficiency into the synchrotron are mainly caused by changes of the cyclotron phase versus radius. Work is going on to study the influence of the cyclotron beam parameters on to the injection efficiency. The phase probe system is a helpful tool for the operator to control the cyclotron performance.

### 3.1.2 Beam Pulsing in the Ion Source Beamline

Pulsing of the beam is necessary for different reasons. The most important is the time structure during the operation of COSY which needs an injection time (i.e. the "beam on"-time) being only a fractional part of the COSY-period time. Typically the injection time will be a few milliseconds in comparison to the period time of some seconds.

Additionally to the "macro-pulsing" a "micro-pulsing" is needed in COSY for diagnostic purposes with time structures in the region of the particle revolution time at injection energy in COSY (2.2 μs); this means typically 1 - 2 μs "beam on"-time and 4 - 40 μs period time. By this way single turns can be injected into COSY and the succeeding revolutions investigated. The beam pulsing is carried out in the source beamline by electrostatic deflection[27].

The trigger electronics generates further trigger and gate signals for several devices in the COSY-system, which have to be synchronized with the beam pulsing, partly with considerable time delay. E.g. the trigger signals for phase measurements in the cyclotron and for loading the injection bumpers in COSY must be available 16 ms before the particle pulse.

The micro-pulsing is active only during the macro"beam on"-time. Due to the gated mode of the micro-pulser the micro-pulses are synchronized to the macro-pulses. The trigger and gate signals of the macro-pulsing are unchanged if the micro-pulsing is enabled.

The time setting of the macro-pulsing is controlled by the COSY-timing system and the pulses for the micro-pulsing are generated by a function generator.

In Figure 1 are shown as an example the micro-pulses and the cyclotron beam pulses measured by a broadband pickup in the injection beamline. The beam pulses are composed from the bunch pulses with 27 MHz-time structure. The beam pulses with negative polarity show an overshoot caused by pulse differentiation due to the high pass behavior of the pickup with 50 Ω-termination.

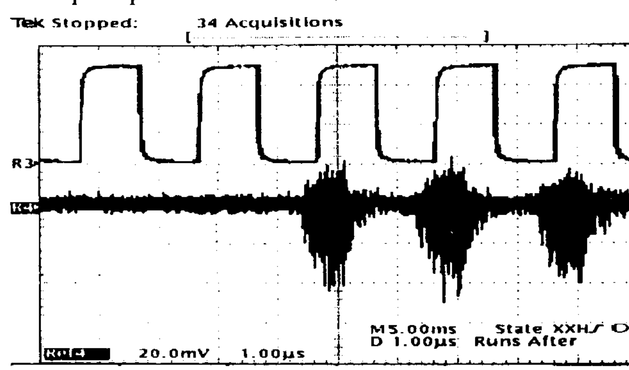


Figure 1: Micro-pulses (upper trace) with 1 μs width and cyclotron beam pulses (lower trace). Time scale is 1 μs/div.

### 3.1.3 Measurement of the COSY Injection Energy

The measurement principle is a time of flight measurement within a long straight section in the injection beamline.[28] This method yields absolute energy as it depends on distance and time measurements only. To get the energy it is necessary to measure the velocity $v = L/T$ of one cyclotron bunch between two capacitive pickups at the beginning and end of the straight line, where L is the distance and T is the variable flight time. $T = T_i + T_f$ consists of two parts: The integer part $T_i = N/f$ is defined precisely by the number N of bunches which are aligned between the two pickups simultaneously, and by the time difference 1/f between two bunches, where f is the cyclotron frequency. The fractional part $T_f < 1/f$ is the time difference between an arbitrary signal from the first pickup and the next following signal from the second pickup. The absolute energy is derived from the formula: $E = m_0c^2 \cdot [(1-\beta^2)^{-1/2}-1]$ with $\beta = L/c \cdot T$.

The broadband preamplifiers of the capacitive pickup probes have been replaced by low noise and low cost preamplifiers of our own development, which are based on MMIC-amplifiers from Mini-circuits of type MAR-X. The main specifications are: amplification 50 dB; impedance 50 Ω in/out; bandwidth 20 kHz - 500 MHz/3 dB; eq. input noise 1.5 nV/$\sqrt{\text{Hz}}$ ; 1 Vpp max output level.

A tunneldiode pulsgenerator has been built to supply the preamplifier inputs with 0.5 ns risetime step pulses simultaneously within 50 ps. This allows remote control of the systems integral performance.

The signals are analyzed by the true sampling scope Tektronix TDS-820. This is now used because of two main advantages: the analogue bandwidth of 6 GHz allows to display the genuine pulse shapes and the sample rate of about 70 kS/s at each channel renders two complete 500 points displays of both input signals within < 7 ms. Therefore the energy measurement can be performed now for each injection cycle individually.

A trigger logic for the external trigger input of the TDS-820 scope was developed which accepts the zero crossings of the cyclotron RF frequency as trigger events only during the injection time. Thus walk effects are prevented and the display can not be overwritten by zero events during the long time between consecutive injections. A switch selectable delay allows to shift the trigger start up to 150 µs after the begin of injection to take into account the 60 µs propagation delay of the particles between ion source and first capacitive pickup behind the cyclotron exit.

The scope is connected via GPIB-bus with a HP-715/33 work station where the HP-VEE System (HP's visual engineering environment) and application programs are operating.

From this workstation a virtual instrument display can be exported to every X-Window-terminal within the COSY-LAN area. Figure 2 shows the injection energy measurement display. Typing the time difference into the DELTA-t field as measured between the maxima (or zero crossing points) of the probe signals by cursor settings, yields the energy of $H_2^+$-ions or protons, respectively. The so obtained kinetic energy is consistent with values derived from cyclotron scaling laws.

The error of the energy measurement is mainly defined by the error of the flight time. The relative error of the energy measurement amounts to about 0.2 %. The contribution from the flight distance can be neglected (in our case L = 26.070 m ± 0.003 m).

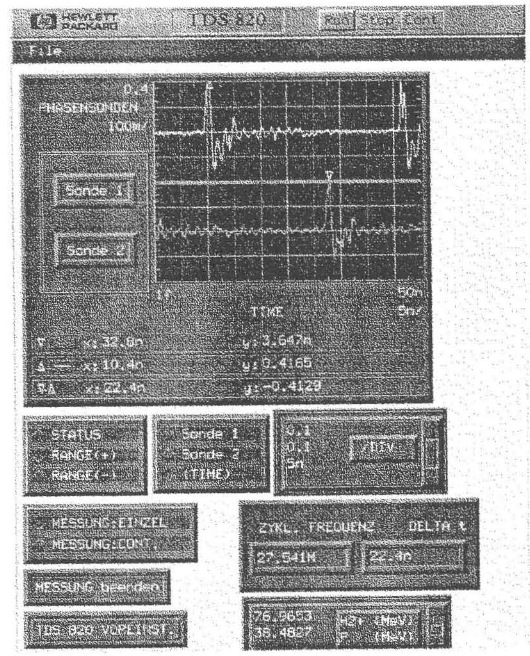


Figure 2: VEE display of the energy measurement with a 5 µA $H_2^+$-beam.

### 3.1.4 Fast Current Measurements of the COSY Injection Beam

The standard instruments for beam current measurements in the injection beamline are Faraday cups and grids, with large response times of > 0.5 ms, but high resolution < 1 %. The COSY-injection current is normally a pulse of some ms width for each cycle, whose time dependence during the first 200 µs should be known. For first turn diagnostic purposes with the beam position monitors the injection current is pulsed with up to 500 kHz. Thus there is need for a fast current monitor with a response time < 200 ns.[29] The capacitive pickup probes as used for the energy measurement, meet this requirement if envelope acquisition mode is applied, which is offered by modern digital storage scopes. The figures 3 and 4 show beam current measurements from our first capacitive pickup at the exit of the cyclotron. The step function in the upper traces marks the time when the source current is started by a deflector which is positioned between the ion-source and cyclotron entrance. The curves below show the envelope of the current signals. Figure 3 is measured with buncher switched off. The current shows some smaller variations within the first 200 µs until it becomes constant. Figure 4 is measured with buncher on. The current shows large and fast variations within the first 200 µs until it becomes constant. The efficiency of the buncher is easily derived from the amplitude relations after 200 µs. The current instabilities at the beginning with buncher on could not be understood until now. The broad baseline of the enveloped current signal comes partly from noise but

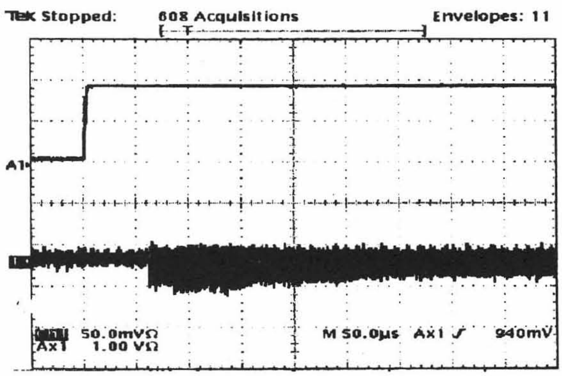


Figure 3: Enveloped cyclotron bunches from a capacitive pickup at the exit of the cyclotron showing moderate current variations in the buncher off mode.

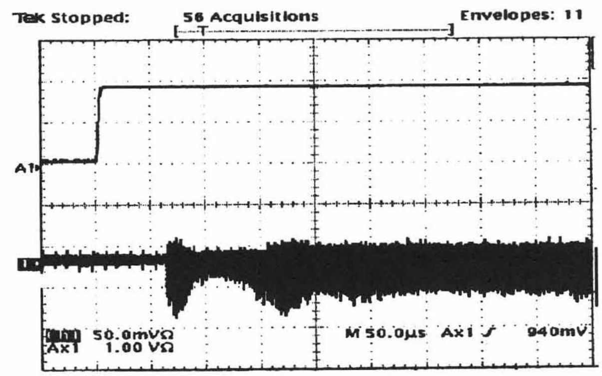


Figure 4: As Fig. 3 in the buncher on mode.

mainly from cross talk of the cyclotron high frequency to the first capacitive pickup. The figures also show the propagation time of about 60 µs of the $H_2^+$ -ions through the cyclotron.

The calibration of the capacitive pickups with Faraday cup results allows the non-beam disturbing measurements of the beam transmission in the injection beamline.

### 3.1.5 Emittance Measurement in the Injection Beamline of COSY

For emittance measurements of the extraced cyclotron beam a computer controlled beam emittance analyzer from NTG (Neue Technologien GmbH) is installed in the straight direction of the first bending magnet.[30]

The emittance measurement is based on a horizontally and vertically moveable slit/detector-system that moves through the beam. The detector system consists of 50 µm thick tantalum strips isolated by 280 µm thick $Al_2O_3$ plates. The resolution of position is determined by the width of the slit (0.1 mm). The achievable resolution in divergence is determined by the width of the detector strips and the drift space length between slit and detector (0.05 mrad standard mode).

The emittance measuring device can be provided with a trigger signal to measure dc and pulsed beams. Typical measured values for a 76 MeV/5 µA $H_2^+$-beam extracted from the cyclotron are 6 $\pi$ mm mrad for the vertical emittance (80 % area in the (x, x')-plane) and twice the value for the horizontal emittance. Two peaks can sometimes be observed in the measured density distribution of the 2-dimensional vertical phase space due to the multiturn extraction in the cyclotron.

The emittance analyzer is designed for measurements of positively charged ions. To measure the emittance of negatively charged ions like $H^-$ a 25 µg/cm² thick carbon foil (diameter 60 mm) is placed in front of the slit for stripping.

The increase of divergence due to scattering in the foil was estimated to 0.2 mrad[31]. Figure 5 shows the measured density distribution in the 2-dimensional horizontal phase space and the angular profile with and without stripping foil. The agreement between estimated and measured increased beam divergence due to the stripping foil is very good.

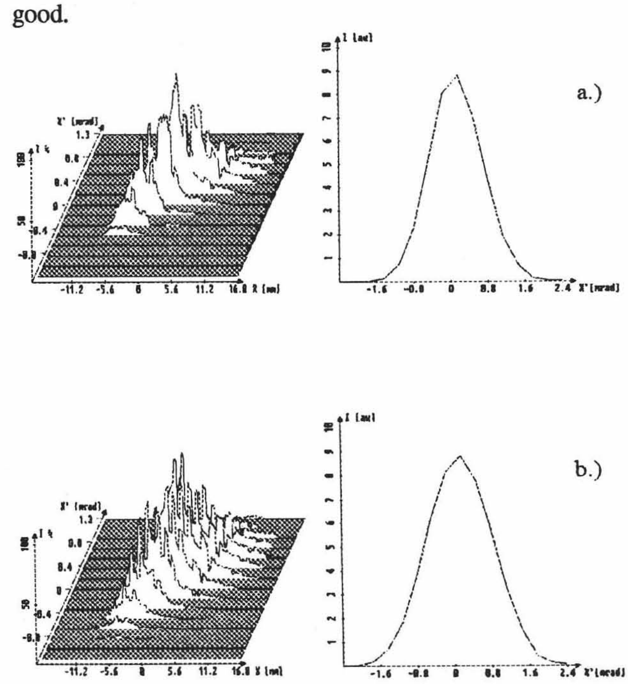


Figure 5: Density distribution in the 2-dimensional horizontal phase space and angular profile a) without and b) with stripping foil.

### *3.2 Cooler Synchrotron Diagnostics*

### 3.2.1 Beam Position Monitor System

The beam position monitor system (BPM) is the backbone of the diagnostics in the COSY ring. In addition a sensitive beam current transformer, a broadband wall current monitor and two resonant tuned Schottky pickups (horiz. and vert.) are installed.

The BPMs are especially used for closed orbit (horizontal and vertical) and tune measurements. For these purposes 29 BPMs are assembled in COSY, with round cross section (∅ 150 mm) in the straight lines and rectangular ones ($150 \cdot 60\ mm^2$) in the bending sections. The BPMs are electrostatic pickups consisting of two electrode pairs (each 130 mm long) rotated by 90° to each other and provided for horizontal and vertical beam position measurements.

Each electrode pair consists of a diagonally cut cylinder or rectangular tube, respectively. By this the electrode signals become linearly dependent on beam position and the sum ($\Sigma$)-signal proportional to the beam intensity independent of beam position. The difference ($\Delta$)-signal is proportional to the amount of deviation of the beam from the central position. The sensitivity of the electrode signals is proportional to the number of particles per bunch and inversely proportional to bunch length and electrode capacity.

The BPM-electronics consist of the preamplifiers, analog and digital moduls (Figure 6). A description of the electronics in detail is given in reference[32].

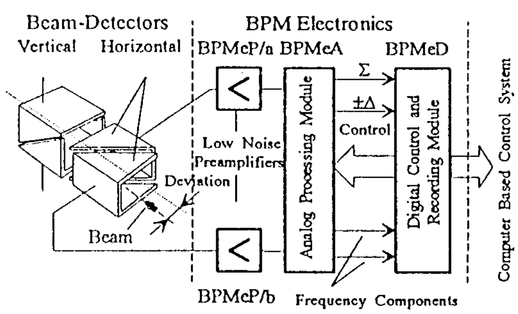


Figure 6: Beam Position Monitor Electronics Assembly.

The low-noise voltage sensitive preamplifiers with high impedance inputs are directly connected to the monitor electrodes. The analogue processing and the digital control and recording modules are housed in a compact and well shielded case (VXI-crate) at about 1.5 m distance inside the accelerator tunnel.

The digitized signals are transferred via local area network to the COSY control room. For control and test-purposes selected signals can be transmitted via coaxial cables into the control room to signal analyzing devices like scopes, spectrum analyzers and so on. The measurements can be done either in the broadband or in the narrowband mode.

The broadband mode with 7 MHz bandwidth (time domain) reproduces the bunch shape and is used for the analysis of the beam turn by turn, e.g. for the analysis of the bunch shape ($\Sigma$-signal) or of beam oscillations ($\Delta$-signal or $\Delta/\Sigma$-quotient) in the acceleration ramp and by kick-excitation. The position accuracy in this case is 0.4 mm. The narrowband mode (frequency domain) with remote presettable bandpass filter bandwidths of 10,100 and 300 kHz in the 0.2 - 60 MHz frequency range results in much higher resolution and, at the same time, in averaging over several turns due to the filter response time. It is used in diagnostic measurements during usual synchrotron operation, e.g. for the closed orbit measurements. The position accuracy is less than 0.1 mm.

The selection of mode, filter bandwidths and wanted amplification are done very comfortable by using the graphical user interface of COSY control system. At the same graphical display also digitized signals can be seen and they can be stored for further investigation.

Figure 7 shows a narrowband measurement of the corrected closed orbit.

In order to get information about the behavior of the first injected turns (first turn analysis), the injected cyclotron beam was pulsed using the micropulsing system (1 µs long pulses every 100 µs). At injection energy the revolution time in COSY is about 2.2 µs. By doing so the BPM signals can be analyzed either in the broadband mode or in the narrowband mode (at 27 MHz of cyclotron beam bunch structure).

Obtained signals from turn to turn by pulsing the injected cyclotron beam was used quite intensively during the startup period of COSY.

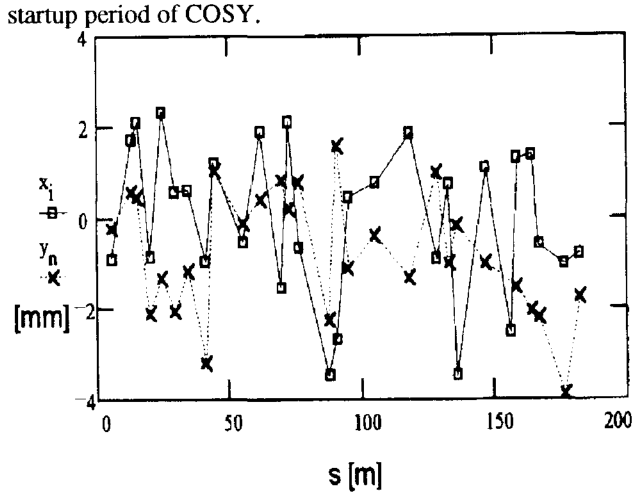


Figure 7: Narrowband measurement of the corrected closed orbit in the horizontal (x) and vertical (y) plane along the ring.

### 3.2.2 Optimization of Extraction Efficiency

For the resonant extraction process at COSY, the horizontal tune is moved towards a third order resonance and the particles are shifted towards the electrostatic septum by a local closed orbit bump. By exciting one or more sextupoles, in addition a phase space boundary (separatrix) with a triangular shape characteristic of the resonance is created. The correct orientation of this separatrix at the location of the electrostatic septum is essential for getting a good extraction efficiency.

In the following measurements of phase space conditions at the position of the electrostatic septum are presented.

The experimental procedure started with a single bunch being horizontally kicked with various angular deflection strengths by a pulsed deflecting magnet (kicker).

The purpose of this fast diagnostic kicker magnet is to excite the beam particles to collective transverse oscillations, which run with betatron frequency and, e.g., are used for the determination of the tune or for phase space investigations. By means of the kicker magnet the beam bunch is short-time (0.75 - 2 μs width; rise- and falltime < 1 μs) deflected and the resulting beam bunch position oscillations are measured using the BPMs. The kicker excitation is synchronized with respect to the COSY-RF signal and can be adjusted in time by programmable delay, so a unique deflection of the total bunch can be performed (bunch synchronous excitation). The installed kicker magnet can be used for horizontal beam deflection only.

From the BPM-electrode signals the amplified and filtered $\Sigma$-and $\Delta$-signals are deduced and digitized by flash-ADCs (20 MHz clock-rate). The results are stored in FIFO-memories. In this way the data of 200 (with 4K FIFO-length) or of 3200 (with 64K) successive turns are recorded.

The beam-centroid displacement (the betatron motion) was measured turn-by-turn with two BPMs located near the electrostatic septum (phase advance much different from $n \cdot \pi$). The conjugate variable of the displacement x, namely $p_x = \alpha x + \beta x'$, is a function of the $\alpha$- and $\beta$-function values at the BPMs, the betatron phase advance between the monitors and the measured displacement $x_1$ and $x_2$ in both monitors. Figure 8 shows transverse phase space plots (first hundred turns) for operation near the third order resonance for different angular deflections. With increasing angular deflection the horizontal tune changes to higher values. A minimum value of the tune spread was observed when the tune is close to the third order resonance (plot with $Q_x$ = 3.669). This is in contrast to the fact, that the betatron motion decoherent time is inversely proportional to the kicked amplitude[33]. In the case of a seventh order resonance an increasing tune spread by increasing kick-amplitude was found. The measured oscillating amplitudes decrease due to Landau damping from turn to turn. If the Landau damping is numerically taken out for all four cases the so corrected amplitudes fill a circle with increasing radius as expected.

In addition the studies of motion of the beam centroid after collectively perturbing the beam by a fast kicker and using the data of all BPMs, yield important information about the lattice[34]. This procedure is also useful in the non-linear beam dynamics study. Due to the non-negligible beam size, the interpretation of the experimental results is difficult, especially if the beam center is displaced nearby the separatrix. Parts of the particles are stable here, parts are unstable. The degree to which the beam centroid motion accurately represents the motion of a single particle depends on the emittance of the beam; the smaller the emittance of the beam, the more accurate is its representation of single particle motion. Further limitations are the decoherence of the betatron motion and the crossing of uncontrollable non-linear resonances. Work is going on including experiments with cooled beams.

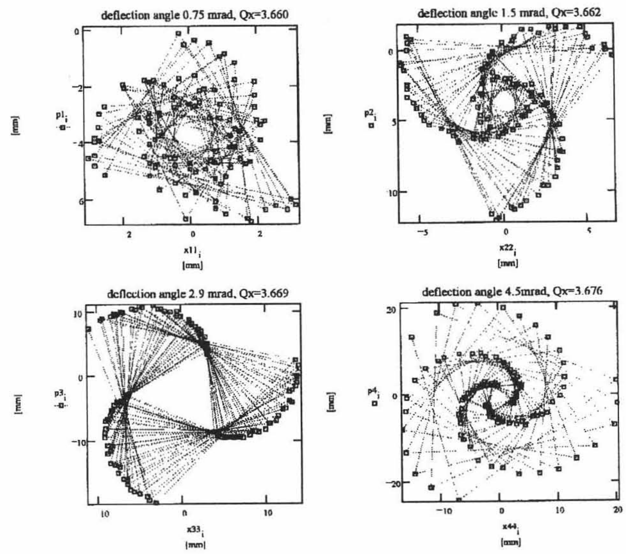


Figure 8: Transverse phase space plots for four different kick amplitudes resulting in the given deflection angles. Proton momentum is 800 MeV/c. The straight lines connect the measured data in turn.

### 3.3 *Multi-wire Proportional Chambers in the Extraction Beamlines*

The intensity of the extracted beam is determined by multi-wire proportional chambers (MWPC) in the extraction beamlines, which until now were successfully used for beam profile measurements[35]. Intensity measurement intrinsically consists of two major informations, the absolute current value and its time structure. Unfortunately the extracted intensity at COSY lays in the range between $10^5$ pps and $10^9$ pps, corresponding to currents of about 0.1 and 100 pA. Thus it is too high for single particle counting and too low for Faraday cup measurement with current amplifier. Ionisation chambers with high sensitive current amplifiers are suitable in this range, but are due to the low cutoff frequency not useful to observe intensity fluctuations up to some kHz, which have to be controlled. The MWPCs are the best choice as the intrinsic gas amplification allows to use less sensitive but fast current amplifiers. Profile and fast intensity measurements are therefore possible with the same detector system. The only disadvantage is that the intrinsic gas amplification as a function of the applied high voltage is not sufficiently precise known from any theoretical or empirical formula. Therefore measurements were performed for an absolute calibration of the MWPC-data in dependence of the applied high voltage. The calibration data were taken with 38 MeV protons from the COSY-injector cyclotron and the corresponding calibration curves at the COSY-energies were extrapolated by scaling the primary ionisation in the MWPC using the Bethe Bloch formula for the energy dependence of the specific energy loss.

The improved MWPCs yield the beam profile and intensity (absolute value and its time structure) in the extraction beamlines. From this measurements the extraction efficiency, the emittance and the beamline transmission are determined.

**Acknowledgements**

It is a pleasure to acknowledge the contribution of the colleagues of the COSY-team, especially J. Bojowald, W. Bräutigam, H. Labus, R. Maier and I. Mohos, who participated in the design of the COSY diagnostic system and took part in providing the measurements presented.

I would like to thank G. Cuttone (INFN LNS Catania), G. Riehl and A. Peters (GSI Darmstadt) for valuable informations.

**References**

1. H. Koziol, CAS-CERN Accel. School, Jyväskylä (1992), CERN 94-01, (1994), p.565
2. G. Jackson, Proc. EPAC,Nice (1990), p.196.
3. P. Strehl,GSI-Preprint 94-27 (1994).
4. S. Herb, Proc. DIPAC 2, Travemünde (1995), DESY M-95 07, p.1.
5. Accel. Instr. Workshops,American Inst. of Phys. Conf. Proc. No. 212 (1989), 229 (1990), 252 (1991), 281 (1992), 319 (1993)and 333 (1994).
6. Proc. Workshop on Adv. Beam Instr., Tsukuba (1991), KEK-Proc. 91-2..
7. Proc. Europ. Workshop on Beam Diag. and Instr. for Part. Accel., DIPAC 1,Montreux (1993), CERN PS/93-35 (BD), CERN SL/93-35 (BI) and DIPAC 2, Travemünde (1995), DESY M -95 07.
8. R. Maier et al, contribution to this conference.
9. R. Jung, Proc. DIPAC 1, Montreux (1993), CERN PS/93-35 (BD), CERN SL/93-35 (BI), p.54.
10. F. Marti and S. Snyder, Proc. of the 13th Int. Conf. on Cyclotrons, Vancouver (1992), p.435.
11. G. Cuttone et al, Proc. DIPAC 2, Travemünde (1995), DESY M-95 07, p.84.
12. F. Marti et al, Proc. of the 12th Int. Conf. on Cyclotrons, Berlin (1989),p.268.
13. M. Crescenti and U.Raich, Proc. DIPAC 2, Travemünde (1995), DESY M-95 07, p.66.
14. G. Riehl, Dissertation, Institut für Angewandte Physik, J.W. Goethe Universität Frankfurt, Frankfurt (1992),GSI-Report GSI-93-43.
15. M. Saarstedt, Dissertation, Institut für Angewandte Physik, J.W.Goethe Universität Frankfurt, Frankfurt (1994).
16. G. Riehl et al, Proc. DIPAC 2, Travemünde (1995), DESY M-95 07, p.6.
17. P. Heeg et al, Proc. Beam Instr. Workshop, Vancouver (1994), AIP Conf. Proc. No 333, p.287.
18. A. Peters et al, Proc. DIPAC 1, Montreux (1993), CERN PS/93-35 (BD), CERN SL/93-35 (BI), p.100.
19. A. Peters et al, Proc. DIPAC 2, Travemünde (1995), DESY M-95 07, p.136.
20. W. Barry et al, Proc. 2nd Accel. Instr. Workshop, Batavia (1990), AIP Conf. Proc. No.229, p.48.
21. W. Barry, CEBAF PR-90-024 (1990).
22. R. Rossmanith, Proc. 3rd Accel. Instr. Workshop, Newport News (1991), AIP Conf. Proc. No.252, p.88.
23. A. Stilman, Proc. Beam Instr. Workshop, Vancouver (1994), AIP Conf. Proc. No 333, p.557.
24. F. Majid et al, The Xwpl system (version 1.3, available by anonymous ftp from pascal.math.yale.edu in the directory /pub/ software/xwpl).
25. K. Kennepohl et al, Proc. of the 13th Int. Conf. on Cyclotrons, Vancouver (1992), p469.
26. W. Bräutigam et al, contribution to this conference.
27. J. Bojowald et al, Juel-2590, ISSN 0366-0885 (1993), p.238.
28. E. Brökel et al, Juel-2879, ISSN 0944-2952 (1994), p.197.
29. H. Labus et al, Juel-2590, ISSN 0366-0885 (1993), p.246.
30. J. Dietrich et al, Juel-2590, ISSN 0366-0885 (1993), p.245.
31. Particle Properties Data Booklet, Physics Letters, Vol.75B, No.1 (April 1978), p.79.
32. I. Biri et al, Real Time '93 Conf., Vancouver (1993).
33. S.Y. Lee, Nonlinear Problems in Accelerator Physics, Proc. of Int. Workshop, Berlin (1992), p.249
34. J. Bojowald et al, Proc. DIPAC 2, Travemünde (1995), DESY M-9507, p.87.
35. H. Labus et al, Juel-3035, ISSN 0944-2952 (1995), p.211.